Electronic Supplementary Material (ESI) for Physical Chemistry Chemical Physics.

Supporting Information to Buckybowls as gas adsorbents: binding of gaseous pollutants and their electric-field induced release

Daniel J. Burrill[†] and Daniel S. Lambrecht[*,†,‡]

†*Department of Chemistry, University of Pittsburgh, Pittsburgh, PA 15260*

‡*Department of Chemistry and Physics, Florida Gulf Coast University, Fort Myers, Florida*

E-mail: lambrecht@pitt.edu,dlambrecht@fgcu.edu

Structural Orientations at zero field

Figure S1 shows the optimized structures for all of the systems studied with zero applied field. There are two images for each system: One top-down and another profile. These give insight into the the types of interactions through the adsorbate-adsorbent distance and orientation.

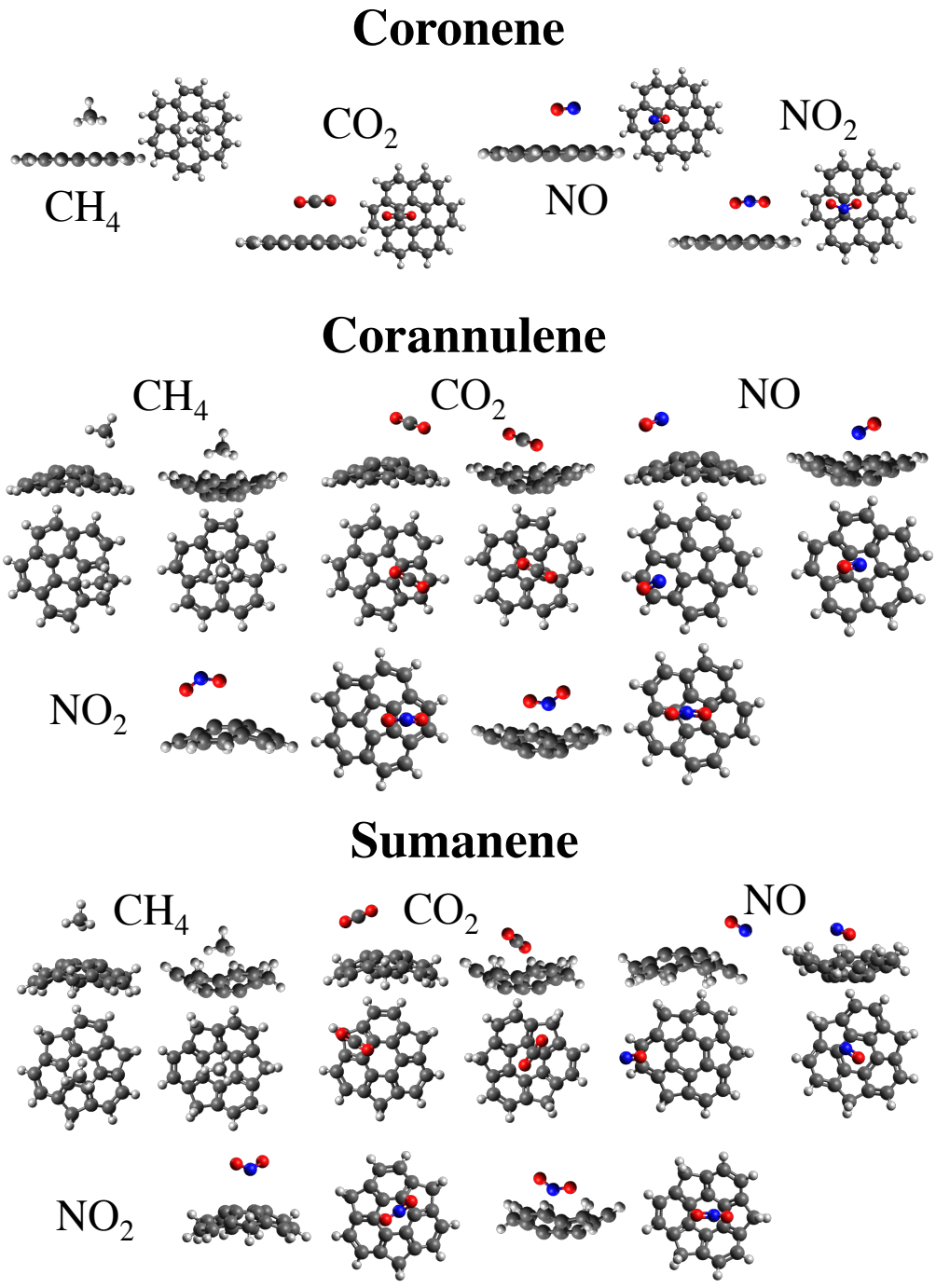

Figure S1: Optimized structures of adsorbents with all adsorbates. Optimizations were carried out with the ωB97X-D/pc-1 level of theory.

Bowl inversion potential energy curve

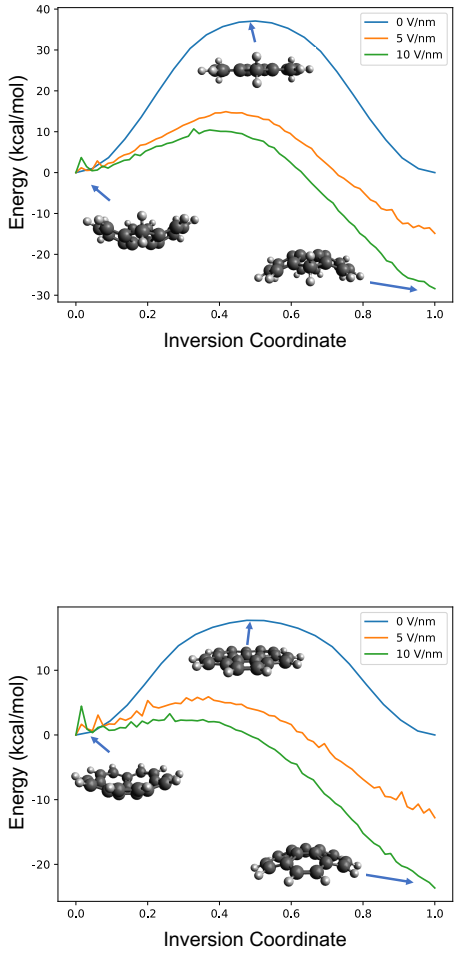

Figure S2: Energy profiles of the bowl inversion for sumanene (top) and corannulene (bottom). Calculations were performed using the freezing string method [1] as implemented in the Q-Chem program package. [2]

Energy decomposition analysis results at zero field

Table S1: Binding energies of adsorbates to sumanene as calculated at the ωB97M-V/pc-2 level within a counterpoise-corrected energy decomposition analysis (all results in kcal/mol).

Adsorbate	Bowl	elec	Pauli	disp	pol	ct	E_{int}
CH_4	BU	-10.93	17.02	-10.07	-0.57	-1.00	-5.56
CO_2	BU	-12.92	18.33	-10.15	-0.79	-0.57	-6.11
NO_2	BU	-13.95	20.42	-10.87	-0.73	-0.92	-6.04
NO	BU	-10.73	16.83	-8.87	-0.47	-1.05	-4.30
CH_4	BD	-4.86	7.89	-4.33	-0.13	-0.39	-1.82
CO_2	BD	-7.30	10.00	-5.04	-0.50	-0.46	-3.29
NO_2	BD	-6.72	10.07	-4.88	-0.26	-0.53	-2.33
NO	BD	-7.75	11.55	-4.48	-0.20	-1.42	-2.29

Table S2: Binding energies of adsorbates to corannulene as calculated at the ωB97M-V/pc-2 level within a counterpoise-corrected energy decomposition analysis (all results in kcal/mol).

Adsorbate	Bowl	elec	Pauli	disp	pol	ct	E_{int}
CH_4	BU	-9.07	14.64	-9.10	-0.49	-0.79	-4.82
CO_2	BU	-11.19	16.59	-9.16	-0.65	-0.36	-4.77
NO_2	BU	-12.44	18.75	-9.94	-0.64	-0.92	-5.19
NO	BU	-9.00	14.15	-7.79	-0.41	-0.88	-3.93
CH_4	BD	-4.82	7.83	-4.23	-0.14	-0.38	-1.73
CO_2	BD	-6.98	10.17	-5.14	-0.47	-0.54	-2.96
NO_2	BD	-9.59	14.66	-6.28	-0.24	-0.90	-2.35
NO	BD	-7.16	11.28	-4.53	-0.20	-1.47	-2.08

Table S3: Binding energies of adsorbates to coronene as calculated at the ωB97M-V/pc-2 level within a counterpoise-corrected energy decomposition analysis (all results in kcal/mol).

Adsorbate	elec	Pauli	disp	pol	ct	E_{int}
CH_4	-6.00	10.03	-6.15	-0.22	-0.60	-2.94
CO_2	-7.79	11.62	-6.58	-0.51	-0.47	-3.71
NO_2	–	–	–	–	–	-3.43[a)]
NO	–	–	–	–	–	-2.38[a)]

[a)] The EDA analysis for NO and NO2 on coronene did not converge despite several attempts. We therefore report the supermolecular binding energy as obtained at the ωB97M-V/pc-2 level of theory.

Energy decomposition analysis with applied electric field

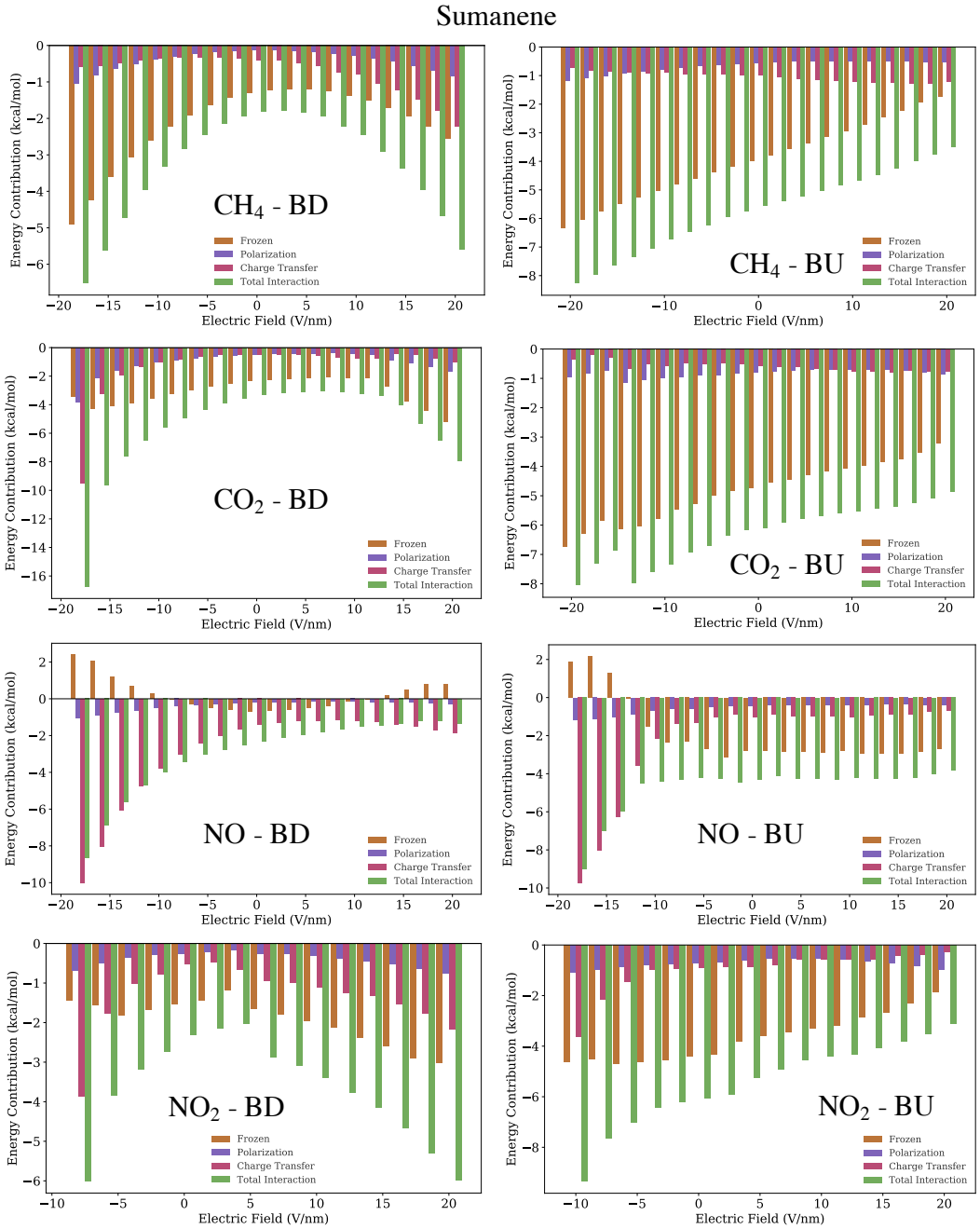

Figure S3: Energy decomposition analysis of sumanene with the various adsorbates. The decomposition is broken down into the frozen, polarization, and charge transfer components along with the total interaction energy.

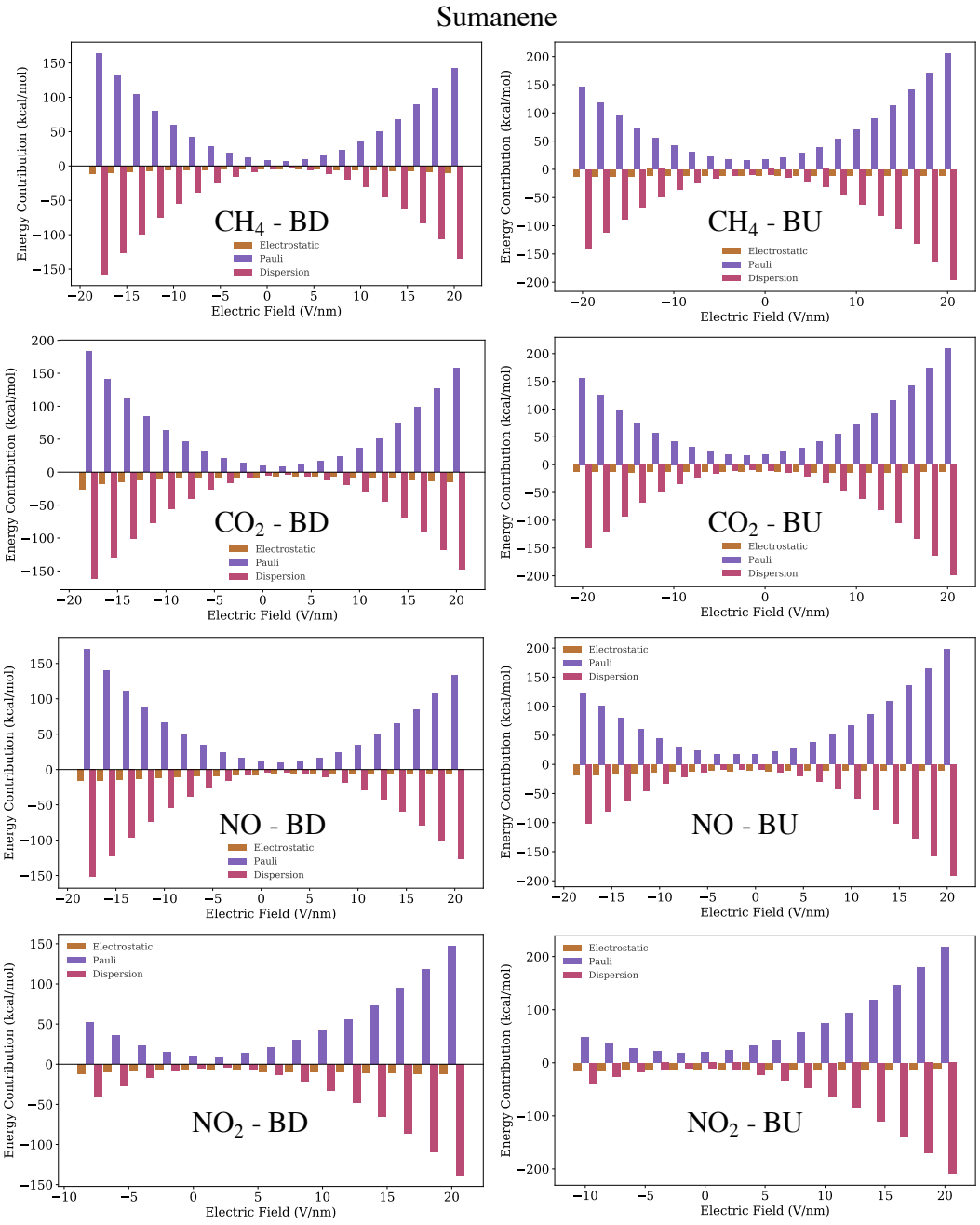

Figure S4: Frozen component of the energy decomposition analysis for sumanene. Electrostatics, dispersion, and Pauli repulsion are shown as the contributions to the frozen component.

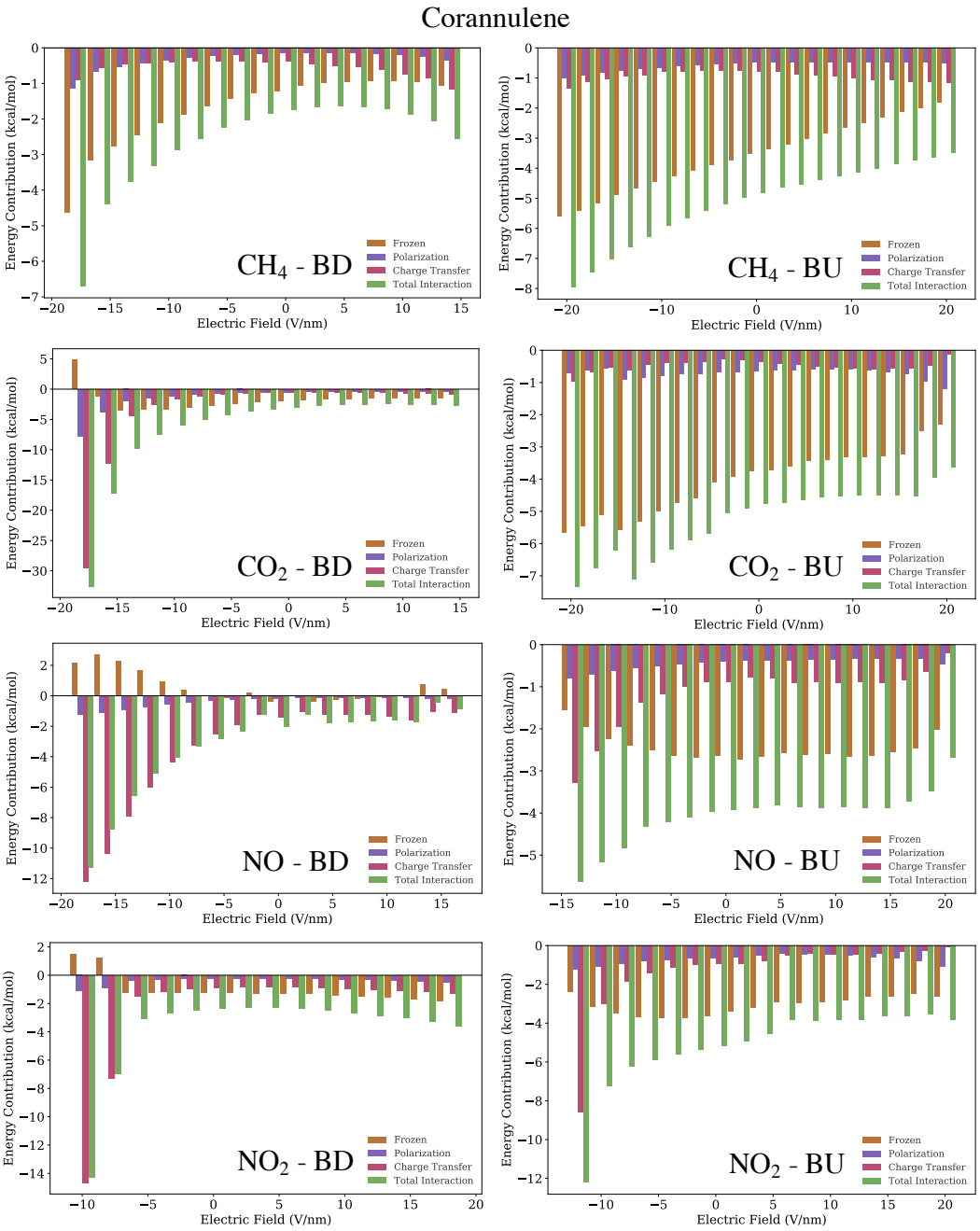

Figure S5: Energy decomposition analysis of corannulene with the various adsorbates. The decomposition is broken down into the frozen, polarization, and charge transfer components along with the total interaction energy.

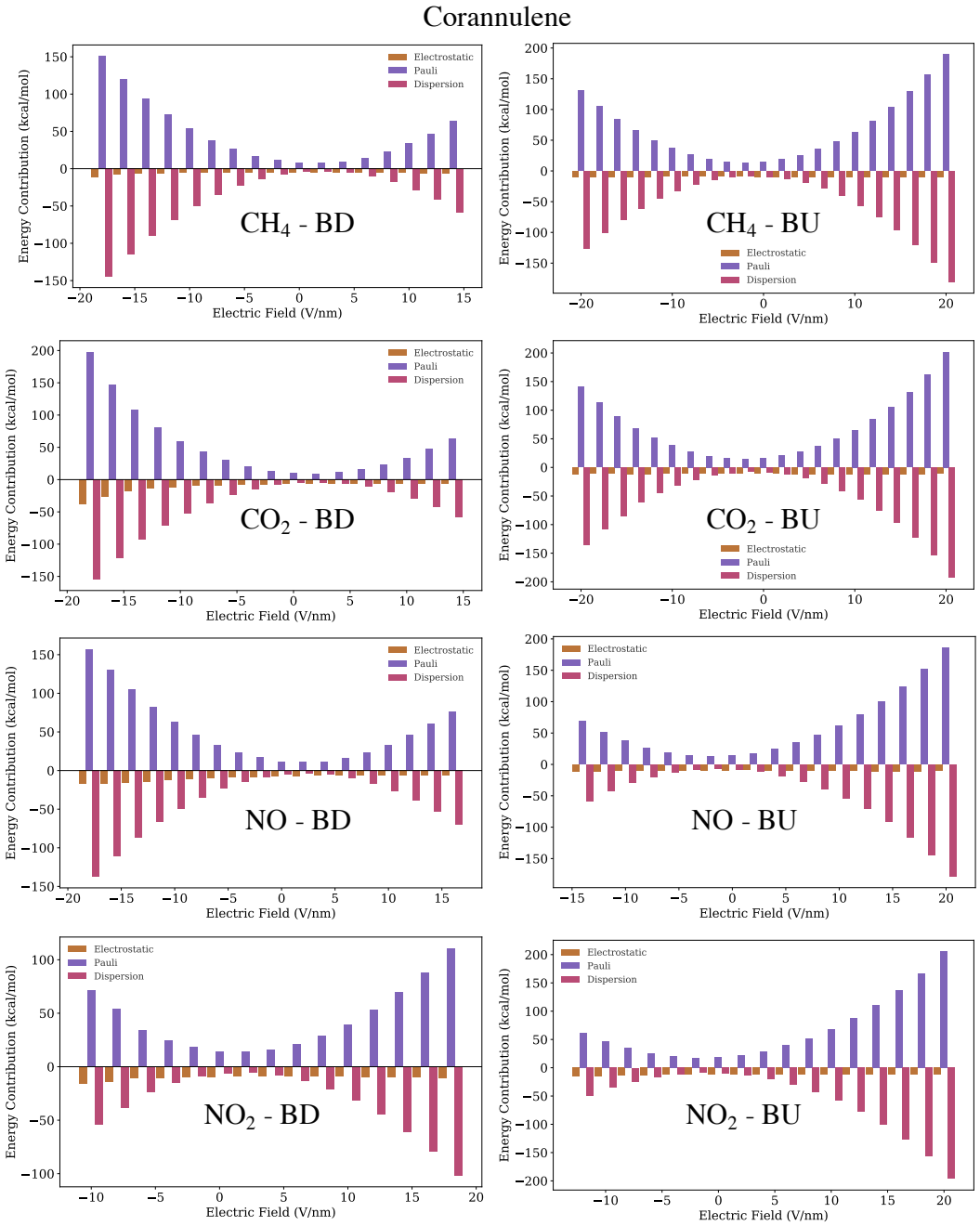

Figure S6: Frozen component of the energy decomposition analysis for corannulene. Electrostatics, dispersion, and Pauli repulsion are shown as the contributions to the frozen component.

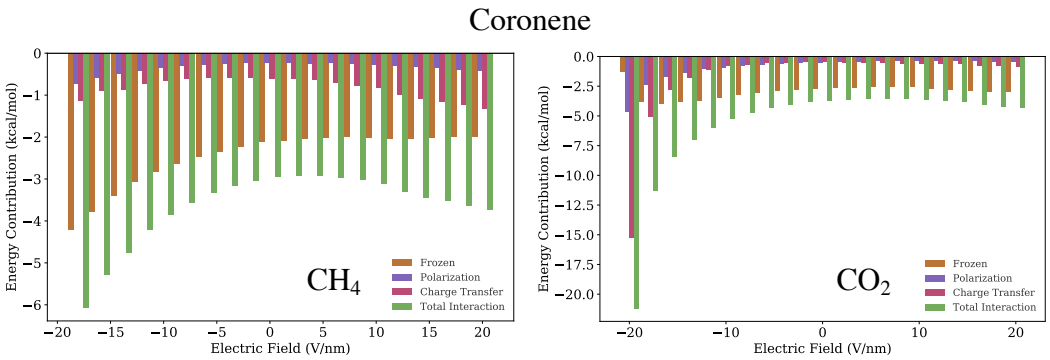

Figure S7: Energy decomposition analysis of coronene with the various adsorbates. The decomposition is broken down into the frozen, polarization, and charge transfer components along with the total interaction energy.

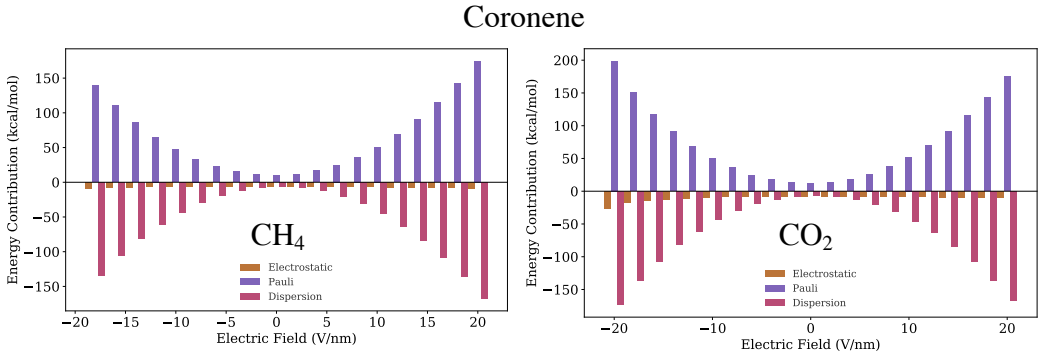

Figure S8: Frozen component of the energy decomposition analysis for coronene. Electrostatics, dispersion, and Pauli repulsion are shown as the contributions to the frozen component.

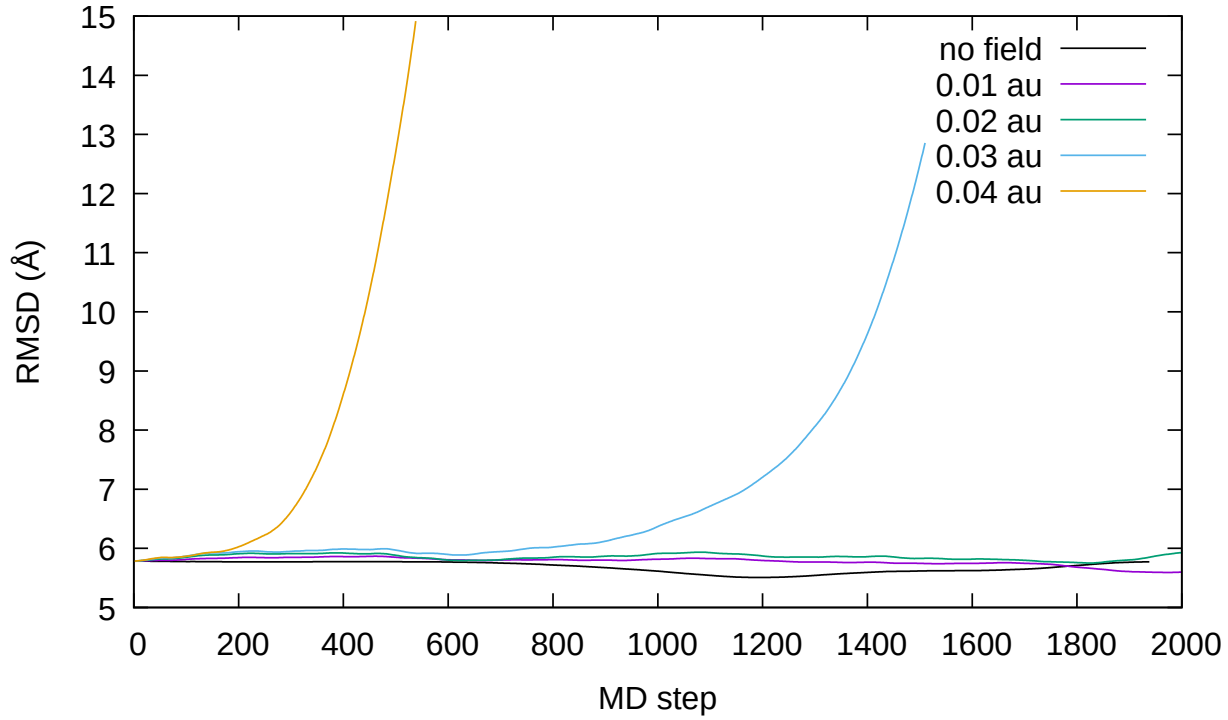

Figure S9: Detachment of NO from sumanene depending on applied electric field strength. Shown is the root mean square distance between NO and the sumanene atoms during molecular dynamics trajectories at a temperature of 1 K and with step size 0.48 fs.

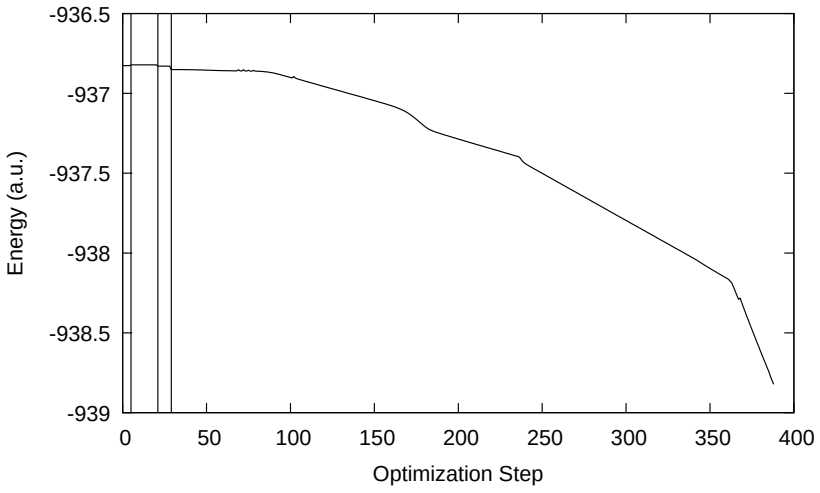

Figure S10: Total energy of NO-sumanene during the course of a geometry optimization as a function of field strength (zero, 0.01, 0.02, and 0.03 a.u. indicated by vertical bars). The total energy remains approximately stable for field strengths from zero to 0.02 a.u., in agreement with observations that there is negligible charge transfer and detachment between NO and sumanene. At field strength 0.03 a.u., excess negative charge is transferred from sumanene into NO, increasing the system's total dipole moment and leading to energetically favorable dipole-field interactions. As the NO detaches, the dipole increases further, leading to energetic stabilization due to favorable dipole-field interactions. This electrostatic picture explains the driving force for charge separation and desorption.

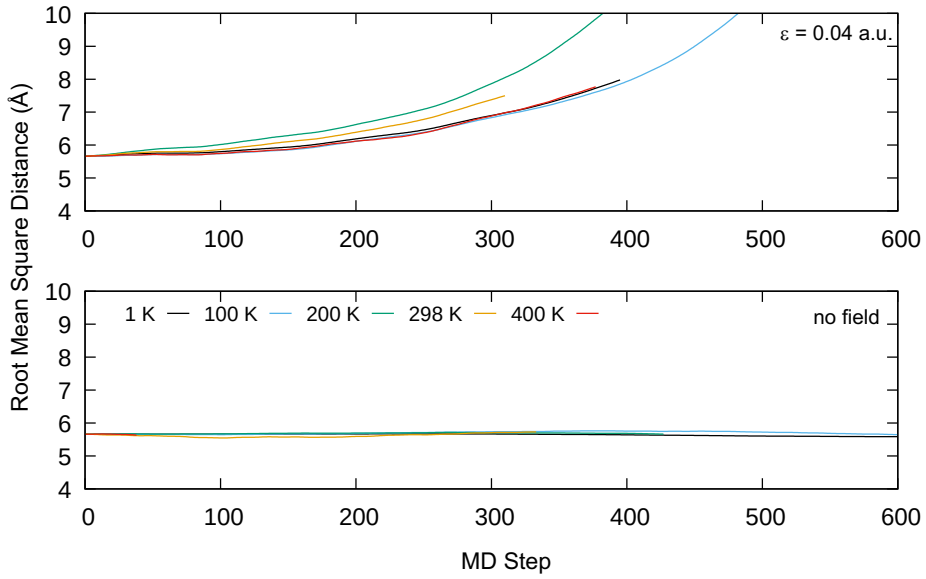

Figure S11: Temperature-dependent molecular dynamics simulation of NO from corannulene. Shown is the root mean square distance of the adsorbate relative to the Buckybowl. Ending trajectories indicates that the trajectory ended early due to self consistent field convergence issues at the last geometry.

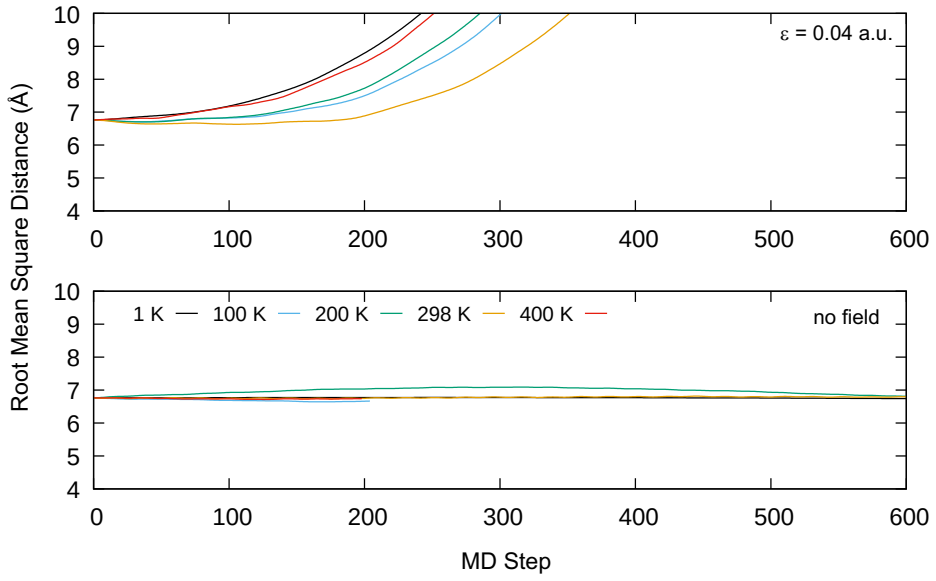

Figure S12: Temperature-dependent molecular dynamics simulation of NO from coronene. Shown is the root mean square distance of the adsorbate relative to the coronene. Ending trajectories indicates that the trajectory ended early due to self consistent field convergence issues at the last geometry.

References

(1) Behn, A.; Zimmerman, P.; Bell, A. T.; Head-Gordon, M. P. Efficient exploration of reaction paths via a freezing string method. *J. Chem. Phys.*

(2) Shao, Y.; Gan, Z.; Epifanovsky, E.; Gilbert, A. T.; Wormit, M.; Kussmann, J.; Lange, A. W.; Behn, A.; Deng, J.; Feng, X. et al. Advances in molecular quantum chemistry contained in the Q-Chem 4 program package. *Molecular Physics* **2015**, *113*, 184–215.